height and molecular rotation (non zero angular momentum) on vibrational mode mixing in triatomic molecules is under investigation.

Acknowledgment. The author thanks Professor Don Secrest of University of Illinois at Urbana-Champaign for several helpful discussions and his kindness to allow me to use Cray Y-MP supercomputer in National Center for Supercomputing Applications(NCSA) on his account. This work was supported in part by the grant from the Korea Science and Engineering Foundation.

References

1. Yamanouchi, K.; Takeuchi, S.; Tsuchiya, S. *J. Chem. Phys.* **1990**, *92*, 4044.
2. Deleon, A.; Jost, R. *J. Chem. Phys.* **1991**, *95*, 5686.
3. Heller, E. J. *J. Chem. Phys.* **1990**, *92*, 1718.
4. Tennyson, J.; Henderson, J. R. *J. Chem. Phys.* **1989**, *91*, 3815.
5. Bačić, Z.; Light, J. C. *J. Chem. Phys.* **1986**, *85*, 4594.
6. Chang, B. H.; Secrest, D. *J. Chem. Phys.* **1991**, *94*, 1196.
7. Natanson, G. A. *J. Chem. Phys.* **1990**, *93*, 6589.
8. Estes, D.; Secrest, D. *Mol. Phys.* **1986**, *59*, 569.
9. Lee, J. S. *J. Chem. Phys.* **1992**, *97*, 7489.
10. Bartholomae, R.; Martin, D.; Sutcliffe, B. T. *J. Mol. Spectrosc.* **1981**, *87*, 367.
11. Simons, G.; Parr, R. G.; Finlan, J. M. *J. Chem. Phys.* **1973**, *59*, 3229.
12. Lee, J. S.; Secrest, D. *J. Phys. Chem.* **1988**, *92*, 1821.
13. Lee, J. S.; Secrest, D. *J. Chem. Phys.* **1986**, *85*, 6565.
14. Lee, J. S.; *Ph. D. Thesis*, University of Illinois at Urbana-Champaign: Urbana, Illinois, U. S. A., **1986**.
15. Renner, R. Z. Physik **1934**, *92*, 172.

Crystal Structures of Fully Dehydrated Zeolite Cd_6-A and of $Rb_{13.5}$-A, the Product of its Reaction with Rubidium, Containing Cationic Clusters

Se Bok Jang, Yang Kim, and Karl Seff*

Department of Chemistry, Pusan National University, Pusan 609-735
**Department of Chemistry, University of Hawaii, 2545 The Mall Honolulu, Hawaii 96822-2275, U.S.A.*
Received October 25, 1993

The crystal structures of Cd_6-A evacuated at 2×10^{-6} Torr and 750°C ($a=12.216(1)$ Å), and of the product of its reaction with Rb vapor ($a=12.187(1)$ Å), have been determined by single-crystal x-ray diffraction techniques in the cubic space group $Pm\bar{3}m$ at 21(1)°C. Their structures were refined to the final error indices, $R_1=0.055$ and $R_2=0.067$ with 191 reflections, and $R_1=0.066$ and $R_2=0.049$ with 90 reflections, respectively, for which $I>3\sigma(I)$. In dehydrated Cd_6-A, six Cd^{2+} ions are found at two different threefold-axis sites near six-oxygen ring centers. Four Cd^{2+} ions are recessed 0.50 Å into the sodalite cavity from the (111) plane at O(3), and the other two extend 0.28 Å into the large cavity from this plane. Treatment at 250°C with 0.1 Torr of Rb vapor reduces all Cd^{2+} ions to give $Rb_{13.5}$-A. Rb species are found at three crystallographic sites: three Rb^+ ions lie at eight-oxygen-ring centers, filling that position, and ca. 10.5 Rb^+ ions lie on threefold axes, 8.0 in the large cavity and 2.5 in the sodalite cavity. In this structure, ca. 1.5 Rb species more than the 12 Rb^+ ions needed to balance the anionic charge of zeolite framework are found, indicating that sorption of Rb^0 has occurred. The occupancies observed can be most simply explained by two "unit cell" compositions, Rb_{12}-A·Rb and Rb_{12}-A·2Rb, of approximately equal population. In sodalite cavities, Rb_{12}-A·Rb would have a $(Rb_2)^+$ cluster and Rb_{12}-A·2Rb would have a triangular $(Rb_3)^+$ cluster. Each of the atoms of these clusters must bind further through a six-oxygen ring to a large cavity Rb^+ to give $(Rb_4)^{3+}$ (linear) and $(Rb_6)^{4+}$ (trigonal). Other unit-cell compositions and other cationic cluster compositions such as Rb_8^{n+} may exist.

Introduction

Complete dehydration of fully Cd^{2+}-exchanged zeolite A had not been achieved. Cd_6-A evacuated at 500°C and 2×10^{-6} Torr for 2 days contains three H_2O molecules per unit cell,[1,2] and temperatures as high as 700°C had not been found to be sufficient to remove all water.[3]

During the past decade, a series of attempts to achieve full Rb^+-exchange of zeolite A had failed.[4,5] Seff *et al.* reported that large monovalent Rb^+ ions exchanged incompletely into zeolite A by flow methods.[4] Only eleven of the twelve Na^+ ions per unit cell were replaced by Rb^+.

Fully dehydrated, fully Rb^+-exchanged zeolite A has been prepared by the reduction of all of the Na^+ ions in dehydrated Na_{12}-A by rubidium vapor.[6] In a series of structures, 12.6 (2) to 13.5(2) Rb species were found per unit cell, more than the twelve Rb^+ ions needed to balance the anionic charge of the zeolite A framework. The structural analyses indicated that dirubidium or trirubidium clusters inside the sodalite cavity coordinate further to rubidium ions in the large cavity

to form $(Rb_4)^{3+}$ and $(Rb_6)^{4+}$ clusters.

This work was done to learn whether fully dehydrated, fully Cd^{2+}-exchanged zeolite A could be prepared and, if so, to determine its structure. This work was also done to learn whether a more stoichiometric Rb-A·Rb structure than had been seen with Na-A or Ca-A might result from treatment of Cd-A with rubidium gas, because cadmium is more easily reduced and can be distilled away from the crystal.

Experimental Section

Crystals of zeolite 4A were prepared by a modification of Charnell's method.[7] Two single crystals about 85 μm on an edge were selected and lodged in separate fine quartz capillaries. An exchange solution of $Cd(NO_3)_2$ and $Cd(O_2CCH_3)_2$ in the mole ratio of 1 : 1 with a total concentration of 0.05 M was allowed to flow past each crystal at a velocity of approximately 1.5 cm/s for 3 days. Each crystal was washed by continuing this procedure using distilled water at 80℃ for 1 h.[2]

Each crystal, still in its fine quartz capillary, was attached to a vacuum system and was cautiously dehydrated by gradually increasing its temperature (*ca.* 25℃/h) to 750℃ at a constant pressure of 2×10^{-6} Torr. Finally, the system was maintained at this state for 48 h. After cooling to room temperature, one crystal (crystal 1), colorless, still under vacuum, was sealed in its capillary by torch. To the second crystal, rubidium vapor was introduced by distillation from a side-arm break-seal ampule to the quartz-tube extension of the crystal-containing capillary. The quartz reaction vessel was then sealed off under vacuum and placed within a pair of cylindrical horizontal ovens, axes colinear, attached. The oven about the crystal was always maintained at a higher temperature than that about the rubidium metal so that rubidium would not distill onto the crystal. The crystal was allowed to react with 0.1 Torr of Rb vapor at 250℃ for 2 h, after which it was sealed off from the reaction vessel by torch after cooling to room temperature. Microscopic examination showed that the crystal (crystal 2) had become black.

X-ray Data Collection

The cubic space group $Pm\bar{3}m$ (no systematic absences) was used instead of $Fm\bar{3}c$ throughout this work for the reasons discussed previously by Seff and Mellum, and references therein.[8,9] Diffraction data were collected with an automated Enraf-Nonius four-circle computer controlled CAD-4 diffractometer equipped with a pulse-height analyzer and a graphite monochromator, using Mo Kα radiation ($K\alpha_1$, $\lambda=0.70930$ Å, $K\alpha_2$, $\lambda=0.71359$ Å). The unit cell constants at 21(1)℃ determined by least-squares refinement of 25 intense reflections for which $18°<2\theta<25°$ are $a=12.216(1)$ Å for crystal 1 and $a=12.187(1)$ Å for crystal 2.

For each crystal, reflections from two intensity-equivalent regions of reciprocal space (*hkl*, $h\le k\le l$ and *lhk*, $l\le h\le k$) were examined. The intensities were measured using the ω-2θ scan technique over a scan width of $(0.80+0.344\tan\theta)°$ in ω. The data were collected using variable scan speeds. Most reflections were observed at slow scan speeds, ranging between 0.24 deg and 0.33 deg min^{-1} in ω. The intensities of three reflections in diverse regions of reciprocal space were recorded after every three hours to monitor crystal and x-ray source stablity. Only small, random fluctuations of these check reflections were noted during the course of data collection. For each region of reciprocal space, the intensities of all lattice points for which $2\theta<70°$ were recorded. Only those of which $I>3\sigma(I)$ were used for structure solution and refinement. This amounted to 191 of the 862 reflections examined for crystal 1, and 90 of the 852 reflections for crystal 2.

The intensities were corrected for Lorentz and polarization effects; the reduced intensities were merged and the resultant estimated standard deviations were assigned to each averaged reflection by the computer programs, PAINT and WEIGHT.[10]

For the first crystal, $\mu R=0.090$, $\rho_{cal}=1.408$ g/cm^3 and F(000)=990; for the second the corresponding values are 0.391, 2.369 g/cm^3 and 1200. The absorption correction was judged to be negligible for both crystals and was not applied.[11]

Structure Determination

Cd_6-A dehydrated at 750℃. Full-matrix least-squares refinement was initiated with the atomic parameters of the framework atoms [(Si, Al), O(1), O(2), and O(3)] of Cd_6-A vacuum dehydrated at 450℃.[12] Anisotropic refinement of the framework atoms converged to an R_1 index, $(\Sigma||F_o|-|F_c||)/\Sigma F_o)$ of 0.46 and a weighted R_2 index, $(\Sigma w(F_o-|F_c|)^2/\Sigma wF_o^2)^{1/2}$ of 0.55.

The initial difference Fourier function revealed one large peak at (0.166, 0.166, 0.166) of height of 9.5(2) eÅ^{-3}. This peak was stable as six Cd^{2+} ions in least-squares refinement. Anisotropic refinement of the framework atoms and Cd^{2+} ions lowered the error indices to $R_1=0.095$ and $R_2=0.085$.

The thermal ellipsoid of the Cd^{2+} position had become very elongated, suggesting the presence of two nonequivalent Cd^{2+} ions at this position. Also, the Fourier function showed this peak to be resolvable into two peaks, which were refined at $x=0.16$ and $x=0.20$ on the threefold axes. Occupancy refinement converged at 2.11(4) and 4.27(4), respectively. These values were reset and fixed at 2.0 and 4.0 Cd^{2+} ions at Cd(1) and Cd(2), respectively, because the cationic charge should not exceed +12 per $Pm\bar{3}m$ unit cell. Anisotropic refinement of the framework atoms and Cd^{2+} ions at Cd(1) and Cd(2) converged to $R_1=0.055$ and $R_2=0.067$ (see Table 1). In the final cycle of least-squares refinement, all shifts in atomic parameters were less than 0.1% of their corresponding standard deviations. The final difference function was featureless except for a peak at (0.0, 0.0, 0.0) of height 2.6(13) eÅ^{-3}. This peak was not within bonding distance of any other atom, and was not considered further.

The 0.50 Å deviation of the ions at Cd(2) into the sodalite unit from the [1, 1, 1] plane at O(3) suggests that water molecules might exist in the sodalite cavity, despite no such indication in Fourier functions. Attempted refinement at several calculated positions for two such water molecules was unsuccessful. Minima in R's were found, but not at positions which afforded acceptable Cd-O or O-O distances. Also the product of the treatment of Cd_6-A dehydrated at 750℃ with Rb(g) (present work) or Cs(g)[13] yielded structures very similar to those of dehydrated Na_{12}-A[14,15] or Ca_6-A[6] treated

Table 1. Positional, Thermal, and Occupancy Parameters[a]

Crystal 1. Fully dehydrated Cd_6-A

Atom	Wyc. Pos.	x	y	z	β_{11}[b]	β_{22}	β_{33}	β_{12}	β_{13}	β_{23}	Occupancy[c] varied	fixed
(Si, Al)	24(k)	0	1833(5)	3683(4)	22(3)	28(3)	22(3)	0	0	3(7)		24.0[d]
O(1)	12(h)	0	2020(20)	5000	50(20)	50(20)	40(10)	0	0	0		12.0
O(2)	12(i)	0	2940(10)	2940(10)	40(10)	31(8)	31(8)	0	0	50(20)		12.0
O(3)	24(m)	1119(6)	1119(6)	3261(9)	37(6)	37(6)	50(10)	10(20)	10(10)	10(10)		24.0
Cd(1)	8(g)	1967(5)	1967(5)	1967(5)	33(3)	33(3)	33(3)	28(8)	28(8)	28(8)	2.11(4)	2.0
Cd(2)	8(g)	1595(3)	1595(3)	1595(3)	42(2)	42(2)	42(2)	41(5)	41(5)	41(5)	4.27(4)	4.0

Crystal 2. $Rb_{13.5}$-A

Atom	Wyc. Pos.	x	y	z	β_{11}[b]	β_{22}	β_{33}	β_{12}	β_{13}	β_{23}	Occupancy[c] varied	fixed
(Si, Al)	24(k)	0	1830(8)	3717(8)	28(7)	36(7)	46(8)	0	0	50(20)		24.0[d]
O(1)	12(h)	0	2300(30)	5000	100(30)	100(30)	20(20)	0	0	0		12.0
O(2)	12(i)	0	2930(20)	2930(20)	30(20)	90(20)	90(20)	0	0	−100(60)		12.0
O(3)	24(m)	1110(10)	1110(10)	3440(10)	60(10)	60(10)	60(20)	−10(40)	50(30)	50(30)		24.0
Rb(1)	3(c)	0	5000	5000	110(20)	150(10)	150(10)	0	0	0	3.12(7)	3.0
Rb(2)	8(g)	2658(3)	2658(3)	2658(3)	91(3)	91(3)	91(3)	45(9)	45(9)	45(9)	7.76(6)	8.0
Rb(3)	8(g)	1000(10)	1000(10)	1000(10)	180(20)	180(20)	180(20)	−80(40)	−80(40)	−80(40)	2.44(8)	2.5

[a] Positional and anisotropic thermal parameters are given $\times 10^4$. Numbers in parentheses are the esd's in the units of the least significant digit given for the corresponding parameter. [b] The anisotropic temperature factor $= \exp[-(\beta_{11}h^2 + \beta_{22}k^2 + \beta_{33}l^2 + \beta_{12}hk + \beta_{13}hl + \beta_{23}kl)]$. [c] Occupancy factors are given as the number of atoms or ions per unit cell. [d] Occupancy for (Si) = 12; occupancy for (Al) = 12.

Table 2. Selected Interatomic Distances (Å) and Angles (deg)

	Cd_6-A	$Rb_{13.5}$-A
(Si, Al)-O(1)	1.62(1)	1.67(2)
(Si, Al)-O(2)	1.63(1)	1.65(2)
(Si, Al)-O(3)	1.70(1)	1.65(1)
Cd(1)-O(3)	2.16(1)	
Cd(2)-O(3)	2.20(1)	
Rb(1)-O(1)		3.29(3)
Rb(1)-O(2)		3.56(1)
Rb(2)-O(3)		2.83(1)
Rb(3)-O(3)		2.98(2)
Rb(1)-Rb(2)		5.18(1)
Rb(2)-Rb(2)		5.71(2)
Rb(2)-Rb(3)		3.50(1)
Rb(3)-Rb(3)		4.21(1) and 3.44(1)
O(1)-(Si, Al)-O(2)	115.7(8)	105(1)
O(1)-(Si, Al)-O(3)	111.8(5)	112.1(9)
O(2)-(Si, Al)-O(3)	105.0(4)	108.3(6)
O(3)-(Si, Al)-O(3)	107.0(4)	110.6(7)
(Si, Al)-O(1)-(Si, Al)	164(1)	139(2)
(Si, Al)-O(2)-(Si, Al)	157.2(6)	161(1)
(Si, Al)-O(3)-(Si, Al)	137.0(7)	146.0(4)
O(3)-Cd(1)-O(3)	118.3(2)	
O(3)-Cd(2)-O(3)	114.9(2)	
O(3)-Rb(2)-O(3)		90.3(4)
O(3)-Rb(3)-O(3)		84.5(2)
Rb(2)-Rb(3)-Rb(3)		180 and 144.7(1)

Numbers in parentheses are estimated standard deviations in the units of the least significant digit given for the corresponding value.

with Rb(g) or Cs(g). This argues that the present crystal of Cd_6-A is fully dehydrated.

Cd_6-A dehydrated at 750°C and treated with Rb vapor. Full-matrix least-squares refinement was initiated with the atomic parameters of the framework atoms [(Si, Al), O(1), O(2), and O(3)] of dehydrated $Rb_{11}Na_1$-A.[4] Anisotropic refinement of the framework atoms converged to an R_1 index of 0.51 and a weighted R_2 index of 0.61.

An initial Fourier synthesis revealed three large peaks: at (0.0, 0.5, 0.5), peak height 30.6(4) $e\text{Å}^{-3}$; at (0.264, 0.264, 0.264), peak height 37.6(3) $e\text{Å}^{-3}$; and at (0.100, 0.100, 0.100), peak height 8.1(3) $e\text{Å}^{-3}$. Anisotropic refinement of the framework atoms and of Rb^+ ions at Rb(1), Rb(2), and Rb(3) converged to $R_1 = 0.072$ and $R_2 = 0.055$ with occupancies of 3.12(7), 7.76(6), and 2.44(8), respectively (see Table 1).

Allowing all occupancies of Rb(i), $i = 1-3$, to vary except that at Rb(1) which was not permitted to exceed 3.0 (its maximum occupancy), and allowing the thermal parameters to refine anisotropically, led to $R_1 = 0.065$ and $R_2 = 0.048$. The occupancy numbers of Rb(i), $i = 1-3$, were reset and fixed as in the last column of Table 1, to give $Rb_{13.5}$-A.

All shifts in the final cycles of least-squares refinement were less than 0.1% of their corresponding standard deviations. The final error indices converged to $R_1 = 0.066$ and

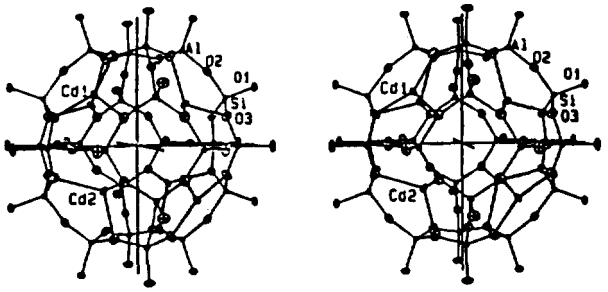

Figure 1. A stereoview of the sodalite unit of fully dehydrated Cd_6-A. Two Cd^{2+} ions at Cd(1) and four Cd^{2+} ions at Cd(2) are shown. Ellipsoids of 20% probability are used.

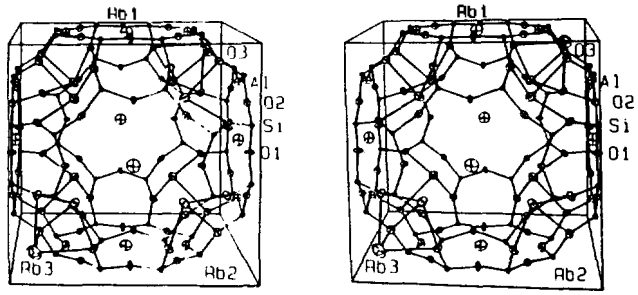

Figure 2. A stereoview of a large cavity in Rb_{13}-A. Eight Rb species at Rb(2), two Rb species at Rb(3), and three Rb^+ ions at Rb(1) are shown. Ellipsoids of 20% probability are used.

$R_2=0.049$. The final difference function was featureless except for a peak 1.1(1) eÅ^{-3} in height at the origin.

For both structures, the full-matrix least-squares program used minimized $\Sigma w(F_o-|F_c|)^2$; the weight (w) of an observation was the reciprocal square of $\sigma(F_o)$, its standard deviation. Atomic scattering factors[16,17] for Cd^{2+}, Rb^+, O^-, and (Si, Al)$^{1.75+}$ were used. The function describing (Si, Al)$^{1.75+}$ is the mean of the Si^0, Si^{4+}, Al^0, and Al^{3+} functions. All scattering factors were modified to account for anomalous dispersion.[18] The final structural parameters and selected interatomic distances and angles are presented in Tables 1 and 2, respectively.

Discussion

Fully dehydrated Cd_6-A. In the crystal structure of vacuum-dehydrated Cd_6-A, all six Cd^{2+} ions associate with 6-ring oxygens on threefold axes. Two ions at Cd(1) and four at Cd(2) per unit cell are 2.16(1) and 2.20(1) Å, respectively, from their respective three O(3)'s (see Figure 1). For comparison, the sum of the conventional ionic radii of Cd^{2+} and O^{2-} is 2.29 Å.[19] Also, the present bonding distances between Cd^{2+} and O(3) are comparable to those in partially dehydrated Cd_6-A.[2,3] In that structure, the Cd-O(3) distance is 2.16(1) Å for three-coordinate Cd^{2+} and 2.23(1) Å for each Cd^{2+} ion which coordinates further to a water molecule. The two Cd^{2+} ions at Cd(1) are recessed 0.28 Å into large cavity from the (111) plane at O(3) (Table 3) and the four Cd^{2+} ions at Cd(2) are correspondingly recessed 0.50 Å into the sodalite cavity. Cd(2) ions arranged tetrahedrally within the sodalite unit and Cd(1) ions occupying two of the remaining 6-rings, is one of several arrangements which minimizes total intercadmium repulsions. If, further, these two groups lie one recessed into the sodalite unit and the other into the large cavity, as is observed, these repulsions are slightly further diminished. Thus it is more favorable electrostatically that six Cd^{2+} ions occupy two different threefold-axis positions as in the present structure (see Table 1).

$Rb_{13.5}$-A. Treating dehydrated Cd_6-A with 0.1 Torr of Rb vapor at 250°C causes all six Cd^{2+} ions to be reduced by Rb atoms. The cadmium atoms produced are no longer found in the zeolite. Instead, Rb^+ ions are found at three crystallographic sites (see Table 1).

Three Rb^+ ions at Rb(1) fill the equipoints of symmetry C_{4v} (D_{4h} in $Pm\bar{3}m$) at the centers of the 8-rings (see Figures 2 and 3), as they have in all previously reported Rb^+-exchanged zeolite A structures.[20,21] Each Rb(1) cation is 3.29(3)

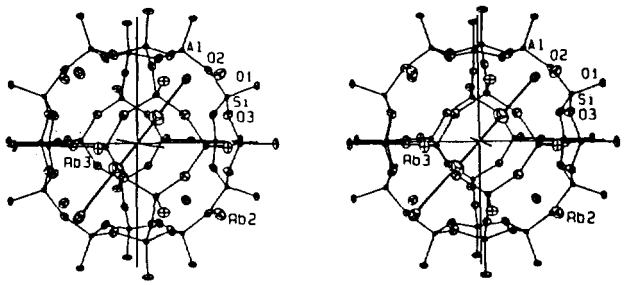

Figure 3. A stereoview of a sodalite cavity in Rb_{13}-A. A linear $(Rb_4)^{3+}$ cluster is shown. Ellipsoids of 20% probability are used.

Tabe 3. Deviations of Atoms (Å) from the (111) Plane at O(3)

	Cd_6-A		$Rb_{13.5}$-A
O(2)	0.27		0.14
Cd(1)	0.28	Rb(2)	1.63
Cd(2)	−0.50	Rb(3)	−1.88

A negative deviation indicates that the atom lies on the same side of the plane as the origin.

Å from four O(1) oxygens and 3.56(1) Å from four O(2)'s (Table 3). These distances are substantially longer than the sum of the ionic radii of O^{2-} and Rb^+, 2.79 Å,[19] as has been discussed before.[20,21]

At Rb(2), 8.0 Rb species are on threefold axes in the large cavity. Each of these extends 1.63 Å into the large cavity from the (111) plane at O(3) (Table 3) and coordinates to three O(3) oxygens of the 6-ring at 2.83(1) Å. At Rb(3), also on threefold axes and associated with 6-rings, 2.5 Rb species are recessed 1.88 Å into the sodalite cavity from the (111) plane at O(3). Each of these ions coordinates to three O(3) oxygens at 2.98(2) Å (see Figures 2 and 3). The sum of the occupancies of the Rb species on the threefold axes is *ca.* 10.5(2).

The product crystal, $Rb_{13.5}$-A, contains more Rb species than are required to balance the anionic charge of the zeolite framework, which is variously estimated to be −11.75[22] to −12.[8] Therefore there are about 1.5 Rb species in excess in $Rb_{13.5}$-A. This excess is attributed to rubidium atom sorption.

The crystal may be viewed as an equal mixture of two kinds of "unit cells", Rb_{12}-A·Rb and Rb_{12}-A·2Rb. Because

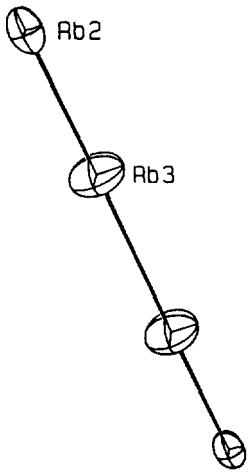

Figure 4. The linear rubidium cluster, $(Rb_4)^{3+}$. Ellipsoids of 20% probability are used.

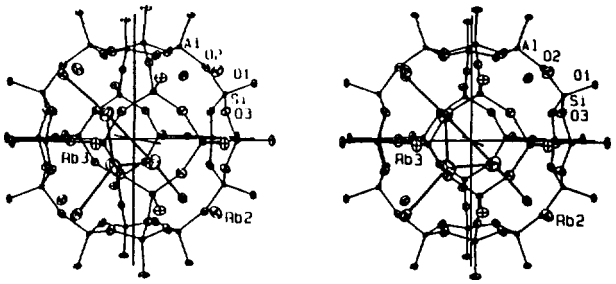

Figure 5. A stereoview of a sodalite cavity in Rb_{14}-A. A trigonal $(Rb_6)^{4+}$ cluster is shown. Ellipsoids of 20% probability are used.

the positions at Rb(2) and Rb(3) must necessarily be averages of the actual positions in unit cells of each composition, some additional uncertainty must be associated with their geometries. It is also possible that these compositions are Rb_{12}-A and Rb_{12}-A·3Rb, or a mixture of all. Rb_{12}-A·3Rb, following the arguments of the next two paragraphs, would contain $(Rb_8)^{n+}$ clusters of symmetry $23=T_d$, where n might be 5 or 6.

The Rb_{12}-A·Rb "unit cell" would have 12.0 Rb^+ ions and one Rb atom. Its sodalite unti with two Rb(3)'s (see Table 1) must have an Rb(3)-Rb(3) distance of 4.21(1) Å (other alternatives, 3.44 or 2.43) are judged to be unnecessarily short), which is quite short as compared to the bond length in Rb metal, 4.95 Å.[23] Each Rb(3) species in the sodalite unit associates with one Rb(2) in the large cavity (Rb(2)-Rb (3)=3.50(1) Å), allowing further electron delocalization. Thus, linear $(Rb_4)^{3+}$ clusters, which lie on threefold axes and extend through the centers of sodalite units (see Figure 3 and 4), have formed. Similar linear $(Cs_4)^{3+}$ clusters were observed in previous studies.[13-15] The bond lengths in this cluster are therefore, from one end to the other, 3.50, 4.21, and 3.50 Å. These are all shorter than those in Rb metal. $(Rb_4)^{3+}$ can be viewed as a one-dimensional particle in a box, four linearly arranged Rb^+ ions with one electron delocalized among them. The length of the box, *ca.* 14.2 Å, is approximated by the sum of the three bond lengths plus twice the ionic radius of Rb^+. A broad absorption transition (1→4)

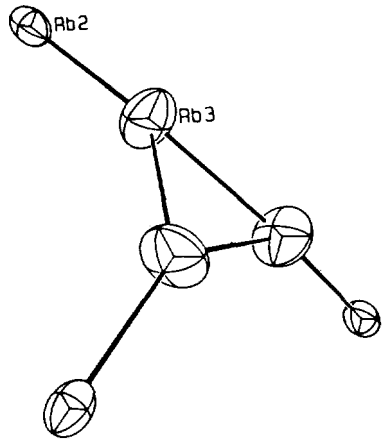

Figure 6. The trigonal rubidium cluster, $(Rb_6)^{4+}$, in Rb_{14}-A. The Rb(3)'s are in the sodalite unit and the Rb(2)'s are in the large cavity. Ellipsoids of 20% probability are used.

is allowed near the middle of the visible range at about 4415 Å, which could account for the black color of the $(Rb_4)^{3+}$-containing crystal.

The Rb_{12}-A·2Rb unit cell would have 12.0 Rb^+ ions and two Rb atoms. Its sodalite unit must have three Rb(3)'s (see Table 1) in each sodalite unit with Rb(3)-Rb(3) distances of 2.43(2) or 3.44(1) Å. The shorter distance is impossibly short, even less than the sum of the radii of two Rb^+ ions, 2.94 Å,[19] and cannot be tolerated. To avoid it, the three Rb(3)'s must form an equilateral triangle with 3.44(1) Å distances (see Figure 5). Three of the eight Rb^+ ions at Rb(2), a filled position, must associate with the Rb(3) triangle in the sodalite unit to allow further electron delocalization. The two electrons from these two Rb^0's per sodalite unit must be delocalized over the shortest Rb-Rb contacts in the structure, those among the three Rb(3)'s in the sodalite cavity and the three Rb(2)'s nearest to these Rb(3)'s, to give the $(Rb_6)^{4+}$ cluster shown in Figures 5 and 6.[6]

Acknowledgement. This work was supported by the Korean Science and Engineering Foundation (Grant No. 921-0300-025-2).

References

1. A discussion of nomenclature is available: (a) Yanagida, R. Y.; Amaro, A. A.; Seff, K. *J. Phys. Chem.* **1973**, *77*, 805; (b) Broussard, L.; Shoemaker, D. P. *J. Am. Chem. Soc.* **1960**, *82*, 1041; (c) Seff, K. *Acc. Chem. Res.* **1976**, *9*, 121.
2. McCusker, L. B.; Seff, K. *J. Am. Chem. Soc.* **1979**, *101*, 5235.
3. McCusker, L. B.; Seff, K. *J. Phys. Chem.* **1980**, *84*, 2827.
4. Firor, R. L.; Seff, K. *J. Am. Chem. Soc.* **1977**, *99*, 1112.
5. Pluth, J. J.; Smith, J. V. *J. Am. Chem. Soc.* **1983**, *105*, 2621.
6. Song, S. H.; Kim, Y.; Seff, K. *J. Phys. Chem.* **1992**, *96*, 10937.
7. Charnell, J. F. *J. Cryst. Growth* **1971**, *8*, 191.
8. Seff, K.; Mellum, M. D. *J. Phys. Chem.* **1984**, *88*, 3560.
9. Riley, P. E.; Seff, K.; Shoemaker, D. P. *J. Phys. Chem.* **1972**, *76*, 2593.

10. Calculations were performed using the *Structure Determination Package Programs* written by Frenz, B. A.; Okaya, Y. Enraf-Nonius, Netherlands, 1987.
11. *International Tables for X-ray Crystallography*, Kynoch: Birmingham, England, 1974; Vol. II, p 132.
12. Koh, K. N.; Kim, U. S.; Kim, D. S.; Kim, Y. *Bull. Korean Chem. Soc.* **1991**, *12*, 178.
13. Jang, S. B.; Kim, Y. *J. Korean Chem. Soc.* **1993**, *37*, 191.
14. Heo, N. H.; Seff, K. *J. Am. Chem. Soc.* **1987**, *109*, 7986.
15. Heo, N. H.; Seff, K. *J. Chem. Soc. Chem. Commun.* **1987**, 1225.
16. Doyle, P. A.; Turner, P. S. *Acta Crystallogr. Sect. A.: Cryst. Phys. Diff. Theor. Gen. Crystallogr.* **1968**, *24*, 390.
17. *International Tables for X-ray Crystallography*, Kynoch: Birmingham, England, 1974; Vol. IV, p 73.
18. Reference 17, p 149.
19. *Handbook of Chemistry and Physics, 70th ed.; Chemical Rubber Co.: Cleveland*, 1989/1990; p F-187.
20. Song, S. H.; Kim, Y.; Seff, K. *J. Phys. Chem.* **1991**, *95*, 9919.
21. Song, S. H.; Ph. D. Thesis, Pusan National University, **1991**.
22. Blackwell, C. S.; Pluth, J. J.; Smith, J. V. *J. Phys. Chem.* **1985**, *89*, 4420.
23. Reference 19, p F-157.

Determination of the Kinetic Energy Release Originating from the Reverse Critical Energy in Unimolecular ion Dissociation

In Chul Yeh, Tae Geol Lee, and Myung Soo Kim*

Department of Chemistry and Research Institute of Molecular Sciences
Seoul National University Seoul 151-742
Received October 29, 1993

A method has been developed to estimate the kinetic energy release originating from the reverse critical energy in unimolecular ion dissociation. Contribution from the excess energy was estimated by RRKM theory, the statistical adiabatic model and the modified phase space calculation. This was subtracted from the experimental kinetic energy release distribution (KERD) via deconvolution. The present method has been applied to the KERDs in H_2 loss from $C_6H_6^{+\cdot}$ and HF loss from $CH_2CF_2^{+\cdot}$. In the present formalism, not only the energy in the reaction coordinate but also the energy in some transitional vibrational degrees of freedom at the transition state is thought to contribute to the experimental kinetic energy release. Details of the methods for treating the transitional modes are found not to be critical to the final outcome. For a reaction with small excess energy and large reverse critical energy, KERD is shown to be mainly governed by the reverse critical energy.

Introduction

There have been considerable interests in the energy disposal in the product regions of unimolecular reactions.[1-4] Statistical models such as the phase space theory[5-8] and the flexible transition state theory[3] have provided good descriptions of the product state distributions for a number of unimolecular reactions going through loose transition states without significant reverse critical energies.[3,5,7-12] In a more general unimolecular reaction with a significant reverse critical energy, there are two distinct components of the internal energy available for partitioning in the products. These are the non-fixed excess energy at the transition state and the reverse critical energy.[1,2,13,14] In this case, further assumptions concerning the dynamics in the exit channel are needed to formulate the energy partitioning within the statistical framework.[15,16] The simplest of such assumptions is, for example, to assign the entire reverse critical energy to the relative translation of the products.[15-17] In most of the cases, however, the experimental kinetic energy release is substantially smaller than the value evaluated under the above assumption.[13,18] This means that some of the reverse critical energy is converted into product vibrations and rotations.[19]

In unimolecular ion dissociation, discussion on the energy partitioning has been limited to the magnitude of the product relative translation.[13,14] This is mainly due to the difficulty in the measurement of vibrational and rotational states of products. Various mass spectrometric techniques have been developed to measure the average of the kinetic energy release (KER) or its distribution (KERD).[13] The average KER or KERD thus obtained is used as a probe in the study of ion structure and fragmentation mechanism.[14] In particular, the fractions of the reverse critical energy released as the relative translational energy of the products in multi-centered elimination reactions have been though to be of diagnostic value in the assignment of transition state geometries.[13,14]

It has long been recognized that the kinetic energy released from the reverse critical energy depends upon the detailed energetics and dynamics of the reaction and is intrinsic to the particular process.[13] A practical difficulty in the meas-

*To whom correspondence should be addressed.